Journal of Hazardous Materials 188 (2011) 357–362

Contents lists available at ScienceDirect

Journal of Hazardous Materials

journal homepage: www.elsevier.com/locate/jhazmat

Decolorization of reactive dye using a photo-ferrioxalate system with brick grain-supported iron oxide

Hui-Pin Cheng[a], Yao-Hui Huang[a,**], Changha Lee[b,*]

[a] Department of Chemical Engineering, National Cheng Kung University, Tainan City 701, Taiwan
[b] School of Urban and Environmental Engineering, Ulsan National Institute of Science and Technology (UNIST), 100 Banyeon-ri, Eonyang-eup, Ulju-gun, Ulsan 698-805, South Korea

ARTICLE INFO

Article history:
Received 18 October 2010
Received in revised form 26 January 2011
Accepted 29 January 2011
Available online 4 February 2011

Keywords:
Fenton reaction
Iron oxide
Reactive Black 5
Ferrioxalate
Decolorization
UV irradiation

ABSTRACT

The photocatalytic activity of a brick grain-supported iron oxide (denoted as B1) was tested for its activity to degrade Reactive Black 5 (RB5) in the presence of oxalic acid. B1 was obtained as a solid waste from a wastewater treatment plant, and characterized using scanning electron microscopy (SEM), energy dispersive X-ray spectroscopy (EDS), X-ray powder diffraction (XRD) and N_2 adsorption/desorption isotherm analyses. The decolorization experiments were performed in a fluidized bed reactor with aeration under UV-A irradiation (λ = 365 nm). The effects of various factors such as solution pH, concentration of oxalic acid and dissolved oxygen on the decolorization of RB5 were evaluated considering the contributions of adsorption and photo-catalytic degradation. The role of dissolved iron in the removal of RB5 and the stability of B1 were also examined. In addition, the removal of TOC during the photo-catalytic reaction was monitored.

1. Introduction

Dye effluents from printing, dyeing and textile industries may contain chemicals that exhibit carcinogenicity, reproductive and developmental toxicity, as well as neurotoxicity and chronic toxicity toward humans and animals [1]. Several methods have been used to treat dye wastewater, such as biodegradation, activated carbon adsorption and chemical coagulation. However, these conventional methods suffer from a few limitations or drawbacks related to cost, efficiency and secondary pollution [2].

Advanced oxidation processes (AOPs) that rely on the highly reactive oxidant, hydroxyl radical (•OH), can be used as alternative technologies for the treatment of wastewater contaminated by reactive dyes. In the last couple of decades, AOPs have attracted considerable attention as emerging technologies for the treatment of nonbiodegradable organic contaminants. In particular, AOPs based on the iron-catalyzed decomposition of hydrogen peroxide (H_2O_2) (i.e. the Fenton system) have been intensively studied mainly for the purposes of wastewater treatment [3,4].

Among the various Fenton systems developed to date, the heterogeneous systems using iron oxides have an advantage over the homogeneous systems, in that the separation of catalysts after the treatment is simple. The separation of dissolved iron in the homogeneous Fenton systems requires additional processes, such as membrane filtration, adsorption or coagulation/precipitation, which poses additional costs and cause secondary pollution. However, heterogeneous Fenton systems usually exhibit lower activity for the production of •OH than the homogeneous Fenton systems. For this reason, many investigators have recently attempted to combine heterogeneous Fenton systems with ultraviolet (UV) irradiation to enhance the activity of Fenton process [5–8]. In particular, the use of oxalate, as a chelating agent for iron, greatly enhances the photo-catalytic activity of the Fenton systems (i.e., the photo-ferrioxalate system). The photo-ferrioxalate system can also produce •OH without the supply of H_2O_2 (Refer to Section 2 for more details).

In this study, a brick grain-supported iron oxide (B1) was tested as a novel heterogeneous photo-catalyst. This material was obtained as a solid waste from an industrial wastewater treatment plant in Taiwan, where the traditional dark Fenton system was used. The objective of the present study was to assess the potential for B1 for the removal of a reactive dye in the photo-ferrioxalate system without an external supply of H_2O_2. Therefore, the decolorization of Reactive Black 5 (RB5) was examined by investigating the factors affecting the system efficiency. The effect of the homo-

* Corresponding author. Tel.: +82 52 217 2812; fax: +82 52 217 2809.
** Corresponding author. Tel.: +886 6 2757575 62636; fax: +886 6 2344496.
E-mail addresses: yhhuang@mail.ncku.edu.tw (Y.-H. Huang), clee@unist.ac.kr (C. Lee).

0304-3894/$ – see front matter © 2011 Elsevier B.V. All rights reserved.
doi:10.1016/j.jhazmat.2011.01.131

geneous reaction due to soluble iron species dissolved from the catalyst was also evaluated.

2. Chemistry of the photo-ferrioxalate system

The photolysis of ferrioxalate produces •OH without the addition of H_2O_2 as the H_2O_2 is formed as an intermediate during the photochemical reactions, via the reduction of dissolved oxygen [9–12]. The mechanism through which •OH is formed during the photolysis of ferrioxalate is briefly summarized as follows.

The primary process of the photolysis of ferrioxalate generates ferrous ion (Fe^{2+}) and oxalyl radical anion ($C_2O_4^{-\bullet}$) (reaction (1)), which subsequently undergoes a rapid decarboxylation to form a carbon dioxide radical anion ($CO_2^{-\bullet}$) (reaction (2)).

$$Fe(C_2O_4)_3^{3-} + h\nu \rightarrow Fe^{2+} + 2C_2O_4^{2-} + C_2O_4^{-\bullet}$$
$$\phi = 1.0\text{–}1.2 \text{ at } 254\text{–}442 \text{ nm [12]} \quad (1)$$

$$C_2O_4^{-\bullet} \rightarrow CO_2 + CO_2^{-\bullet} \quad (2)$$

The fate of $CO_2^{-\bullet}$ depends on the competitive reactions between dissolved oxygen and ferrioxalate (reactions (3) and (4)). At relatively low ferrioxalate concentrations, $CO_2^{-\bullet}$ reacts with oxygen to produce a superoxide radical anion ($O_2^{-\bullet}$) (reaction (4)), which can be either reduced further to H_2O_2 by the reaction with Fe^{2+} (reaction (5)) or oxidized back to oxygen by the reaction with ferrioxalate (reaction (6)).

$$CO_2^{-\bullet} + O_2 \rightarrow CO_2 + O_2^{-\bullet} \quad (3)$$

$$CO_2^{-\bullet} + Fe(C_2O_4)_3^{3-} \rightarrow Fe^{2+} + CO_2 + 3C_2O_4^{2-} \quad (4)$$

$$O_2^{-\bullet} + Fe^{2+} + 2H^+ \rightarrow Fe^{3+} + H_2O_2 \quad (5)$$

$$O_2^{-\bullet} + Fe(C_2O_4)_3^{3-} \rightarrow Fe^{2+} + 3C_2O_4^{2-} + O_2 \quad (6)$$

The H_2O_2 produced via these reactions is converted into •OH via the well-known Fenton reaction (reaction (7)).

$$Fe^{2+} + H_2O_2 \rightarrow Fe^{3+} + OH^- + {}^\bullet OH \quad (7)$$

3. Materials and methods

3.1. Reagents

All chemicals were of reagent grade and used without further purification. Doubly distilled and deionized water was used for preparing all solutions. The purity of RB5 (Fig. 1a; M.W. = 991.82) reagent used in this study was 55%, but the ash content was not taken into account when calculating the concentration of RB5. Stock solutions of oxalic acid (100 mM) and RB5 (1 mM) were prepared and stored under dark conditions. RB5 (Refer to the chemical structure in Fig. 1a) exhibited a visible absorption peak at 597 nm in the pH range of 3–11.5.

3.2. Preparation of B1

A novel catalyst of iron oxide supported on brick grains was obtained as a solid waste from a wastewater treatment plant located in Taichung County, Taiwan. The plant employs the Fenton process (the Fe^{2+}/H_2O_2 system) with a biological pre-treatment step to treat textile dyeing wastewater, and brick grains to reduce the generation of iron sludge from the Fenton treatment.

The general process of the plant and the procedure for obtaining B1 are as follows. The bioeffluents from dyeing wastewater and Fenton's reagent (H_2O_2 and $FeSO_4$) were continuously fed into the bottom of a cylindrical fluidized bed reactor (1 m diameter × 7 m height) packed with brick grains. The molar ratio of H_2O_2 to $FeSO_4$ fed into the reactor was controlled at 2:1. The ferric species produced from the Fenton reaction were immobilized onto the surfaces of brick grains, gradually forming iron oxide layers. The brick grains coated by iron oxide were withdrawn from the reactor after 3 month of operation (denoted as B1). The particle size and density of B1 were approximately 1 mm in diameter and 2.53 g/cm^3, respectively.

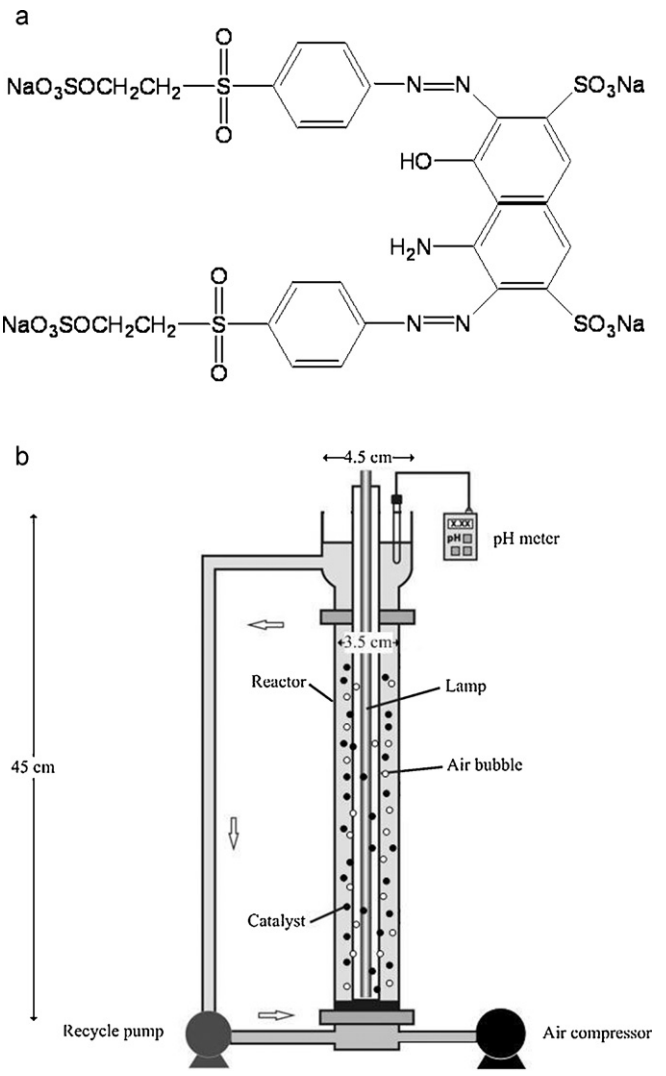

Fig. 1. (a) Chemical structure of RB5 and (b) schematic diagram of the three-phase fluidized bed reactor.

3.3. Characterization of B1

The morphologies of the brick grain support and B1 were obtained using a scanning electron microscope (SEM; JEOL JSM-6700F). The atomic composition of B1 surface was measured using energy dispersive spectra (EDS; Oxford INCA-400). The X-ray diffraction pattern was obtained using a powder diffractometer (Rigaku RX III), with Cu K-α radiation (accelerating voltage 40 kV; current 30 mA). The specific surface area of B1 was analyzed using N_2 adsorption/desorption BET isotherms. The iron content of B1 was determined to be 27.4% by analyzing the Fe ions dissolved from an acidified aliquot of the material, using an atomic absorbance spectrophotometer (SensAA; GBC) [13].

3.4. Experimental setup and procedure

The experiments on the removal of RB5 were performed in a cylindrical three-phase fluidized bed reactor (3.5 cm diameter × 45 cm height), equipped with a 15W black light blue (BLB) lamp (λ_{max} = 365 nm) (Fig. 1b). The lamp was covered by a Pyrex jacket tube to allow light of $\lambda > 320$ nm. A pH meter was placed on the upper end of the reactor to continuously monitor the solution pH. Compressed air was bubbled from the reactor bottom to suspend B1 and maintain good mixing conditions. In some experiments, ultrapure nitrogen gas was used for deaeration.

RB5 solution ($[RB5]_0$ = 20 μM) was prepared and placed in the reactor, with a predetermined quantity of B1 and oxalic acid added. The pH of the solution was initially adjusted to a predetermined value and maintained within ±0.2 units during the entire experiment using dilute solutions of HNO_3 and NaOH. The experiments were initiated by turning on the lamp. During the first 120 min after the initiation of the photochemical reaction, the lamp was turn off, with the solution pH raised to 11.5 by the addition of NaOH to desorb the organic compounds from the surface of B1 (The pH_{zpc} of B1 is 7.5). Samples were periodically withdrawn, and filtered through a 0.45 μm polyvinylidene fluoride membrane prior to analysis.

3.5. Analytical methods

The decolorization of RB5 was analyzed by measuring the visible light absorbance at 597 nm, using a UV–vis spectrometer (Jasco 7850). An atomic absorption spectrometer (Z-6100, HITACHI) was used to measure the dissolved iron in solution. Analysis of Fe(II) was carried out using 1,10-phenanthroline [14]. The concentration of oxalate was measured with potassium permanganate via titration [15]. TOC was analyzed using a SIEVERS 900 analyzer. The samples for the TOC measurement were pretreated by acidification (using phosphoric acid), followed by aeration to remove any inorganic carbon.

Table 1
Surface atomic compositions of the brick grain and B1 using EDS.

Element	Brick grain (at.%)	B1 (at.%)
C	17.82	33.59
O	52.73	43.50
Fe	3.96	19.44
Al	8.95	1.74
Si	16.54	1.73

4. Results and discussion

4.1. Surface properties of B1

Table 1 presents the surface chemical compositions of the brick grain support and B1 determined by EDS. The SEM images of the brick grain support and B1 (Fig. 2a and b) indicate that the originally rough surface of the brick grain support had been smoothed due to the iron oxide coating from the 3 months of reaction in the plant. The XRD analyses demonstrated that the brick grain support exhibits characteristic peaks of quartz (SiO_2-file number 46-1045, JCPDS), but B1 has no isomorphic phase probably due to the amorphous iron oxide coating (Fig. 2c). The specific surface area of B1 was measured and found to be 158 m^2/g.

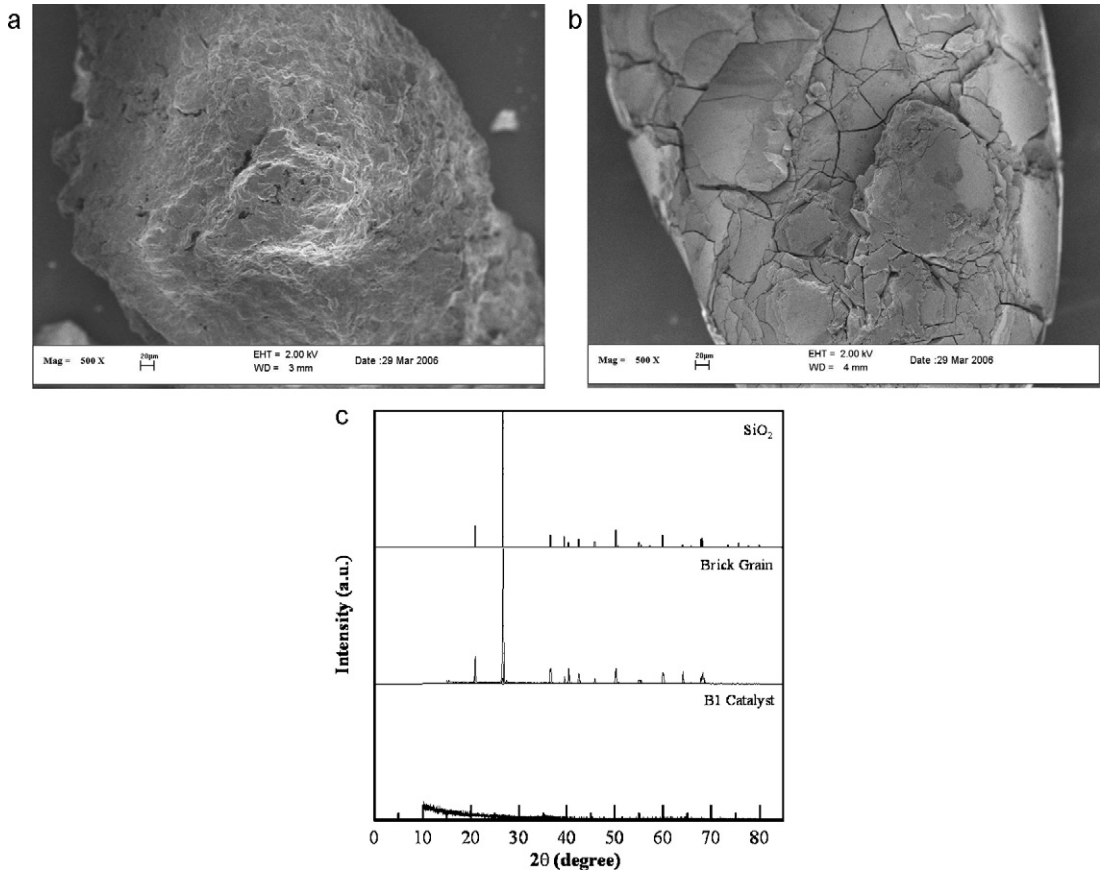

Fig. 2. Scanning electron microscopic images of (a) the brick grain support, (b) B1 (500×), and (c) XRD patterns of B1.

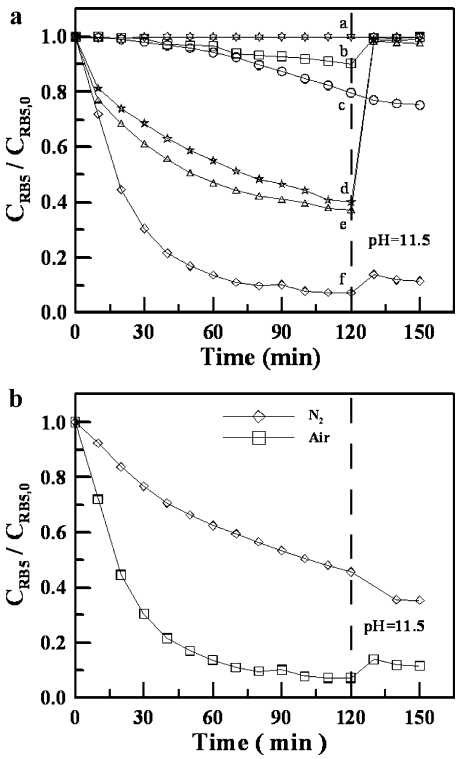

Fig. 3. (a) Decolorization of RB5 under various conditions, with aeration (a: UV alone, b: oxalic acid and B1, c: oxalic acid with UV, d: B1 alone, e: B1 with UV, f: oxalic acid and B1 with UV); (b) Comparison of the decolorization of RB5 between aerated and N_2-saturated conditions ([oxalic acid]$_0$ = 0.33 mM; [B1]$_0$ = 10 g/L; [RB5]$_0$ = 20 μM; pH 5).

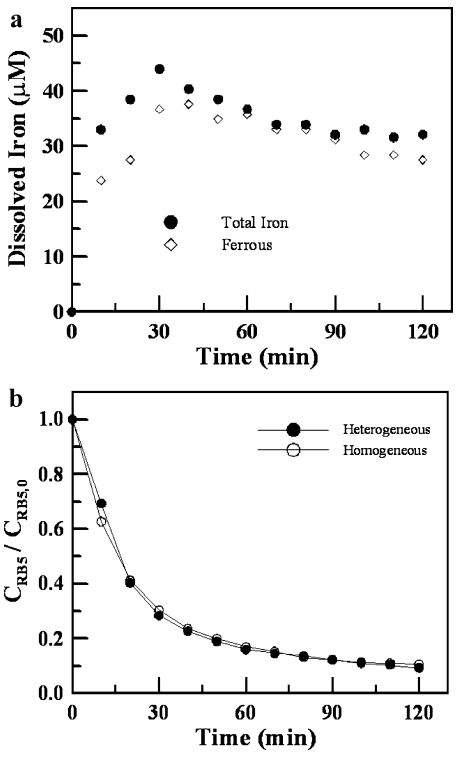

Fig. 4. (a) Concentration of dissolved iron from B1; (b) Comparison of the RB5 decolorization activity between B1 and ferrous ion ([oxalic acid]$_0$ = 0.33 mM; [B1]$_0$ = 10 g/L; [Fe^{2+}]$_0$ = 40 μM; [RB5]$_0$ = 20 μM; pH 5).

4.2. Degradation and adsorption of RB5

The photo-catalytic experiments were carried out for 120 min at pH 5, with the solution pH then raised to 11.5 to desorb RB5 from the surface of B1 (Fig. 3a). The decolorization of RB5 by direct UV photolysis was negligible (curve (a) in Fig. 3a). In the absence of UV light, with 10 g L^{-1} B1 and 0.33 mM oxalic acid (curve b), the RB5 concentration decreased by approximately 10% in 120 min, mainly due to the adsorption of RB5 onto the surface. Without UVA light and 0.33 mM oxalic acid (curve c), limited degradation of RB5 was observed (approximately 20%). No clear explanation can be provided for the degradation of RB5 in curve c, but it may be attributable to the direct electron transfer between the photo-excited state of RB5 and oxalate ions. With 10 g L^{-1} B1 alone (curve d), the RB5 concentration decreased by 60% during 120 min due to adsorption: when the solution pH was raised to 11.5, the absorbance returned to its initial value. The difference between curves b and d indicated that oxalate competes with RB5 for adsorption onto the surface of B1. UV irradiation in the presence of B1 did not significantly influence the decolorization of RB5 (curve e). However, a significant amount of RB5 was removed in the presence of 10 g L^{-1} B1 and 0.33 mM oxalic acid under UV irradiation (curve f). The concentration of RB5 decreased by almost 90% for 120 min, with less than 10% of the initial concentration of RB5 recovered after raising the pH to 11.5, indicating that the removal of RB5 due to adsorption was not significant.

4.3. Degradation of RB5 in the absence of oxygen

The degradation of RB5 under N_2-saturated conditions was compared to that in the presence of oxygen (Fig. 3b). Interestingly, approximately 50% of the initial RB5 was degraded even in the absence of oxygen, indicating that the degradation of RB5 can take place via a reductive pathway. The carbon dioxide radical anions ($CO_2^{-\bullet}$), generated by the photolysis of ferrioxalate complexes, may be responsible for the degradation of RB5 in the absence of oxygen. $CO_2^{-\bullet}$ has a relatively high reducing power ($E_H^0[CO_2/CO_2^{-\bullet}] \approx -1.9$ V [16]), and has been reported to be capable of degrading several organic contaminants [17–19]. In the presence of oxygen, $CO_2^{-\bullet}$ is rapidly consumed by its reaction with oxygen (reaction (3)).

4.4. Role of dissolved iron

The catalytic processes with heterogeneous iron catalysts involve the reactions that occur on the surface of the catalyst as well as those in the bulk phase due to soluble iron dissolved from the catalyst. Several reports have shown that both the heterogeneous and homogeneous reactions significantly contribute to the degradation of the target compounds in the photo-catalytic systems using iron oxides [20–23]. On the contrary, only a few studies have reported on the degradation of dye compounds, and shown a negligible effect of the homogeneous reactions due to dissolved iron species [24,25].

To examine the contribution of dissolved iron in our system, the concentration of iron leaching from B1 was monitored throughout the reaction (Fig. 4a). The total dissolved iron and ferrous ions were measured by an atomic absorption spectrometer and phenanthroline method, respectively. The concentration of total dissolved iron increased to 45 μM during the initial 30 min assisted by complexation of surface iron with oxalate, and then gradually decreased to approximately 35 μM at 120 min as the concentration of oxalate decreased (Fig. 7). In addition, most of the dissolved iron was present as ferrous ions.

In order to evaluate the effect of dissolved iron on the degradation of RB5, the decolorization of RB5 by the homogeneous system,

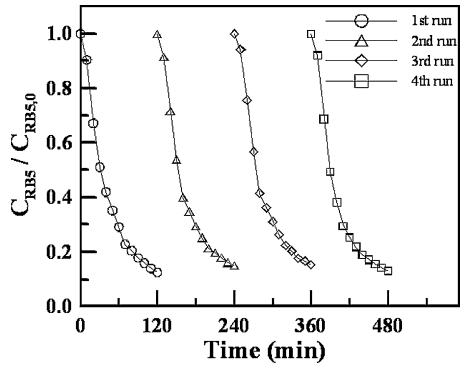

Fig. 5. Decolorization of RB5 by multiple reuse of B1 ([oxalic acid]$_0$ = 0 33 mM; [B1]$_0$ = 10 g/L; [RB5]$_0$ = 20 μM; pH 5).

using 40 μM Fe(II) (the amount comparable to that of the dissolved ion from B1), was examined by comparing the result to that with the heterogeneous system using B1 (Fig. 4b). As a result, no difference was found between the two systems, indicating that the dissolved ferrous ions from B1, rather than the surface reactions of the material, are predominantly responsible for the photocatalytic degradation of RB5. In fact, •OH can be formed via the iron-oxalate complexes present on the surface of B1. However, in the presence of oxalic acid, RB5 is not adsorbed on the B1 surface to a significant extent curve b in Fig. 3a), and thereby •OH produced in the vicinity of the surface may not be used in the RB5 degradation.

4.5. Stability of the B1 activity

B1 needs to maintain constant long-term activity for its effective application in the wastewater treatment industry. The stability of the activity of B1 was examined by conducting multiple runs reusing B1 under identical reaction conditions (Fig. 5). The degradation efficiency of RB5 was almost the same during the repetitive runs. Although the degradation of RB5 in this system was found to be mainly due to the homogeneous reactions of dissolved iron from B1 (Section 4.4), the amount of iron consumed in each run was negligible relative to the iron content within the material. Assuming that a similar amount of iron (ca. 40 μM) leaches out for each run, the activity of B1 can last for approximately 1200 runs.

4.6. Effects of pH and the concentration of oxalic acid

The decolorization of RB5 was investigated in the pH range 3–7. The rate of RB5 decolorization was slightly higher at pH 4 than at pH 3, but decreased with increasing pH from 4 to 7 (Fig. 6a). The negative effect of pH can be explained by the lesser availability of iron at higher pH values. The formation of Fe(III)-oxyhydroxides under neutral pH conditions may result in surface passivation of B1, lowering the iron dissolution rate. In addition, the dissolved iron (mostly ferrous ion; Fig. 4a) can form insoluble ferrous hydroxide (i.e., $Fe(OH)_{2(s)}$) at above pH 6, inhibiting the Fenton reaction. Indeed, the concentration of total dissolved iron at pH 7 was less than 5 μM at 120 min. Conversely, the faster decolorization at pH 4 than pH 3 may be attributable to the enhanced formation of H_2O_2 at the higher pH value. It has been suggested that the rate-determining step for the production of •OH in the photo-ferrioxalate system, without externally supplied H_2O_2, is the formation of H_2O_2 via the reactions of HO_2•/O_2^{-}• with Fe^{2+} [9]. The reaction of O_2^{-}• with Fe^{2+} (reaction (5); $k_5 = 7.2 \times 10^8\ M^{-1}\ s^{-1}$ [26]) is known to be three orders of magnitude faster than the reaction of HO_2• with Fe^{2+} (reaction (8); $k_8 = 7.2 \times 10^5\ M^{-1}\ s^{-1}$ [27]).

$$HO_2^{\bullet} + Fe^{2+} + H^+ \rightarrow Fe^{3+} + H_2O_2 \quad (8)$$

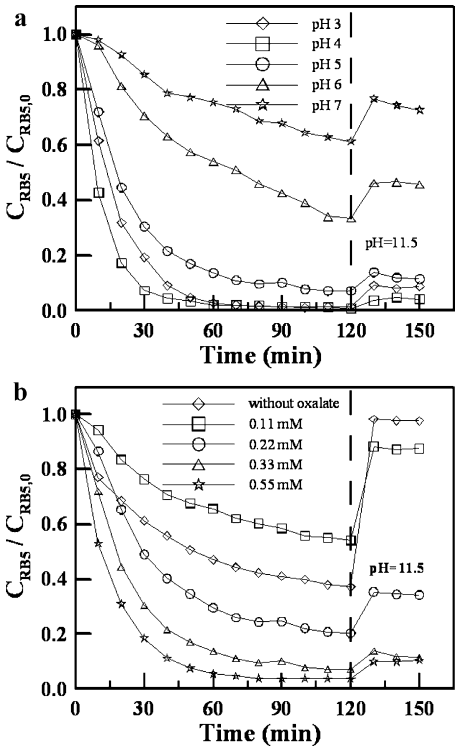

Fig. 6. Effects of (a) pH ([oxalic acid]$_0$ = 0.33 mM; [B1]$_0$ = 10 g L^{-1}), and (b) concentration of oxalic acid ([B1]$_0$ = 10 g L^{-1}; [RB5]$_0$ = 20 μM; pH 5) on the decolorization of RB5.

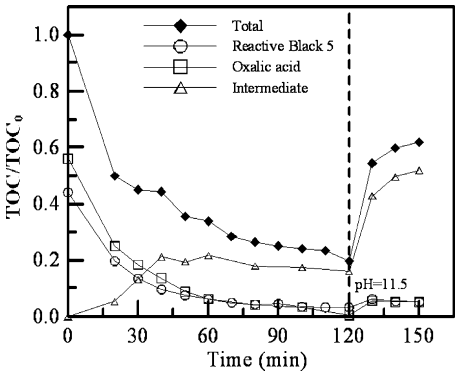

Fig. 7. Variation in total organic carbon (TOC) concentration ([oxalic acid]$_0$ = 0.33 mM; [B1]$_0$ = 10 g L^{-1}; [RB5]$_0$ = 20 μM; pH 5).

The decolorization of RB5 was accelerated with increasing oxalic acid concentration from 0.11 to 0.55 mM (Fig. 6b). In the absence of oxalic acid, RB5 was approximately 60% decolorized in 120 min, mainly due to adsorption: the absorbance was completely returned to the initial value on raising the pH after the reaction. However, it was obvious that the amount of RB5 desorbed from the B1 surface decreased with increasing oxalic acid concentration, indicating that an increased amount of RB5 was removed by the photo-catalytic degradation. With more than 0.33 mM oxalic acid, the removal of RB5 due to adsorption accounted for less than 5% of the total decolorization.

4.7. Mineralization of RB5

TOC was monitored during the photochemical reaction and after desorption by raising pH (Fig. 7). The concentrations of RB5 and oxalic acid were converted into the corresponding TOC values. The TOC values of the intermediates were calculated by subtracting the

values for RB5 and oxalate from the measured TOC values. During the 120 min photochemical reaction, approximately 80% of TOC was removed, but 40% of the initial value was recovered when the pH was adjusted to 11.5 after the reaction. The TOC values of the intermediates after desorption were similar to the initial TOC value for RB5, indicating that the removal of TOC due to oxidative mineralization was negligible. It appears that the removal of TOC during the photochemical reaction mainly resulted from the decomposition of oxalic acid into carbon dioxide and the physical adsorption of RB5 and its intermediates onto the B1 surface.

5. Conclusion

This study demonstrated that a brick grain-supported iron oxide (B1) can be effectively applied for the decolorization of a reactive dye, RB5, by photo-catalytic degradation and physical adsorption. B1 was capable of not only decolorizing RB5, but also removing TOCs from RB5 and its oxidation intermediates. Several factors affected the efficiency of the RB5 decolorization, such as dissolved oxygen, pH and the concentration of oxalic acid. The decolorization of RB5 was greater under aerated than N_2-saturated conditions. However, even in the absence of oxygen, a significant amount of RB5 was decolorized due to the reductive degradation by $CO_2^{-\bullet}$. The increased pH value lowered the rate of RB5 decolorization; whereas, the raised concentration of oxalic acid facilitated the oxidative degradation of RB5. The photo-catalytic degradation of RB5 was attributed to the homogeneous reactions of dissolved iron species rather than the surface reactions, indicating that the activity of B1 lasts only until the initially loaded iron is completely consumed. However, the mineralization of RB5 was mainly due to the physical adsorption of RB5 and its oxidation intermediates onto the surface of B1.

Acknowledgements

The authors would like to thank the National Science Council of the Republic of China for financially supporting this research under Contract No. NSC 98-2221-E-006-282.

References

[1] R. Jain, M. Mathur, S. Sikarwar, A. Mittal, Removal of the hazardous dye rhodamine B through photocatalytic and adsorption treatments, J. Environ. Manage. 85 (2007) 956–964.
[2] A.D. Bokare, R.C. Chikate, C.V. Rode, K.M. Paknikar, Iron-nickel bimetallic nanoparticles for reductive degradation of azo dye Orange G in aqueous solution, Appl. Catal. B: Environ. 79 (2008) 270–278.
[3] B.D. Lee, M. Hosomi, Fenton oxidation of ethanol-washed distillation-concentrated benzo(A)pyrene: reaction product identification and biodegradability, Water Res. 35 (2001) 2314–2319.
[4] J. Fernandez, J. Bandara, A. Lopez, P. Buffat, J. Kiwi, Photoassisted Fenton degradation of nonbiodegradable azo dye (Orange II) in Fe-free solutions mediated by cation transfer membranes, Langmuir 15 (1998) 185–192.
[5] J. Fernandez, M.R. Dhananjeyan, J. Kiwi, Y. Senuma, J. Hilborn, Evidence for Fenton photoassisted processes mediated by encapsulated Fe ions at biocompatible pH values, J. Phys. Chem. B 104 (2000) 5298–5301.
[6] J. Feng, X. Hu, P.L. Yue, H.Y. Zhu, G.Q. Lu, A novel laponite clay-based Fe nanocomposite and its photo-catalytic activity in photo-assisted degradation of Orange II, Chem. Eng. Sci. 58 (2003) 679–685.
[7] J. Feng, X. Hu, P.L. Yue, H.Y. Zhu, G.Q. Lu, Discoloration and mineralization of Reactive Red HE-3B by heterogeneous photo-Fenton reaction, Water Res. 37 (2003) 3776–3784.
[8] C.L. Hsueh, Y.H. Huang, C.C. Wang, C.Y. Chen, Photoassisted Fenton degradation of nonbiodegradable azo-dye (Reactive Black 5) over a novel supported iron oxide catalyst at neutral pH, J. Mol. Catal. A: Chem. 245 (2006) 78–86.
[9] J. Jeong, J. Yoon, pH effect on OH radical production in photo/ferrioxalate system, Water Res. 39 (2005) 2893–2900.
[10] D.L. Sedlak, J. Hoign, The role of copper and oxalate in the redox cycling of iron in atmospheric waters, Atmos. Environ. 27A (1993) 2173–2185.
[11] Y. Zuo, J. Hoigne, Formation of hydrogen peroxide and depletion of oxalic acid in atmospheric water by photolysis of iron(III)-oxalato complexes, Environ. Sci. Technol. 26 (1992) 1014–1022.
[12] V. Balzani, V. Carassiti, Photochemistry of Coordination Compounds, Academic Press, New York, 1970.
[13] U. Schwertmann, R.M. Cornell, Iron Oxides in the Laboratory: Preparation and Characterization, 2nd edition, WILEY-VCH, New York, 1991.
[14] H. Tamura, K. Goto, T. Yotsuyanagi, M. Nagayama, Spectrophotometric determination of iron(II) with 1,10-phenanthroline in the presence of large amounts of iron(III), Talanta 21 (1974) 314–318.
[15] K.A. Kovács, P. Gróf, L. Burai, M. Riedel, Revising the mechanism of the permanganate/oxalate reaction, J. Phys. Chem. A 108 (2004) 11026–11031.
[16] H.A. Schwarz, R.W. Dodson, Reduction potentials of CO_2^- and the alcohol radicals, J. Phys. Chem. 93 (1989) 409–414.
[17] A. Khindaria, T.A. Grover, S.D. Aust, Reductive dehalogenation of aliphatic halocarbons by lignin peroxidase of Phanerochaete chrysosporium, Environ. Sci. Technol. 29 (1995) 719–725.
[18] P.L. Huston, J.J. Pignatello, Reduction of perchloroalkanes by ferrioxalate-generated carboxylate radical preceding mineralization by the photo-Fenton reaction, Environ. Sci. Technol. 30 (1996) 3457–3463.
[19] J. Jeong, J. Yoon, Dual roles of CO_2^- for degrading synthetic organic chemicals in the photo/ferrioxalate system, Water Res. 38 (2004) 3531–3540.
[20] Q. Lan, F. Li, C. Liu, X.Z. Li, Heterogeneous photodegradation of pentachlorophenol with maghemite and oxalate under UV illumination, Environ. Sci. Technol. 42 (2008) 7918–7923.
[21] F.B. Li, X.Z. Li, X.M. Li, T.X. Liu, J. Dong, Heterogeneous photodegradation of bisphenol A with iron oxides and oxalate in aqueous solution, J. Colloid Interface Sci. 311 (2007) 481–490.
[22] M.I. Pariente, F. Martínez, J.A. Melero, J.Á. Botas, T. Velegraki, N.P. Xekoukoulotakis, D. Mantzavinos, Heterogeneous photo-Fenton oxidation of benzoic acid in water: effect of operating conditions, reaction by-products and coupling with biological treatment, Appl. Catal. B: Environ. 85 (2008) 24–32.
[23] F. Gulshan, S. Yanagida, Y. Kameshima, T. Isobe, A. Nakajima, K. Okada, Various factors affecting photodecomposition of methylene blue by iron-oxides in an oxalate solution, Water Res. 44 (2010) 2876–2884.
[24] J. Feng, X. Hu, P.L. Yue, H.Y. Zhu, G.Q. Lu, Degradation of azo-dye Orange II by a photoassisted Fenton reaction using a novel composite of iron oxide and silicate nanoparticles as a catalyst, Ind. Eng. Chem. Res. 42 (2003) 2058–2066.
[25] T. Yuranova, O. Enea, E. Mielczarski, J. Mielczarski, P. Albers, J. Kiwi, Fenton immobilized photo-assisted catalysis through a Fe/C structured fabric, Appl. Catal. B: Environ. 49 (2004) 39–50.
[26] R. Matthews, The radiation chemistry of aqueous ferrous sulfate solutions at natural pH, Aust. J. Chem. 36 (1983) 1305–1317.
[27] T.E. Graedel, M.L. Mandich, C.J. Weschler, Kinetic Model studies of atmospheric droplet chemistry 2. Homogeneous transition metal chemistry in raindrops, J. Geophys. Res. 91 (1986) 5205–5221.